Acta Crystallographica Section D
Biological Crystallography
ISSN 0907-4449

2.0 Å structure of prostaglandin H_2 synthase-1 reconstituted with a manganese porphyrin cofactor

Kushol Gupta,[a]‡ Barry S. Selinsky[b] and Patrick J. Loll[a]*

[a]Department of Biochemistry and Molecular Biology, Drexel University College of Medicine, Philadelphia, PA 19102, USA, and [b]Department of Chemistry, Villanova University, Villanova, PA 19085, USA

‡ Current address: Department of Biochemistry and Biophysics, University of Pennsylvania, Philadelphia, PA 19104, USA.

Correspondence e-mail: pat.loll@drexel.edu

Received 8 September 2005
Accepted 4 November 2005

PDB Reference: Mn^{III}-reconstituted ovine PGHS-1, 2ayl, r2aylsf.

Prostaglandin H_2 synthase (EC 1.14.99.1) is a clinically important drug target that catalyzes two key steps in the biosynthesis of the eicosanoid hormones. The enzyme contains spatially distinct cyclooxygenase and peroxidase active sites, both of which require a heme cofactor. Substitution of ferric heme by Mn^{III} protoporphyrin IX greatly diminishes the peroxidase activity, but has little effect on the cyclooxygenase activity. Here, the 2.0 Å resolution crystal structure of the Mn^{III} form of ovine prostaglandin H_2 synthase-1 is described (R = 21.8%, R_{free} = 23.7%). Substitution of Mn^{III} for Fe^{III} causes no structural perturbations in the protein. However, the out-of-plane displacement of the manganese ion with respect to the porphyrin is greater than that of the iron by approximately 0.2 Å. This perturbation may help to explain the altered catalytic properties of the manganese enzyme.

1. Introduction

Prostaglandin H_2 synthase (PGHS; EC 1.14.99.1) is an integral membrane protein having both cyclooxygenase and peroxidase activities. These two activities sequentially convert arachidonic acid to prostaglandin G_2 and then to prostaglandin H_2; prostaglandin H_2 is transformed by other enzymes into various eicosanoid hormones, including prostacyclin and thromboxane A_2 (Marnett *et al.*, 1999; Smith *et al.*, 1996, 2000). The cyclooxygenase active site of PGHS is the target of nonsteroidal anti-inflammatory drugs (NSAIDs) such as aspirin, ibuprofen, rofecoxib and celecoxib (Simmons *et al.*, 2004).

PGHS contains a ferric heme cofactor that is required for both the cyclooxygenase and peroxidase activities. When reconstituted with metalloporphryins other than Fe^{III}-protoporphyrin IX (PPIX), the enzyme loses one or both activities. For example, reconstitution with Zn-PPIX or Co^{III}-PPIX eliminates both the peroxidase and cyclooxygenase activities (Malkowski *et al.*, 2000; Ogino *et al.*, 1978). When reconstituted with Mn^{III}-PPIX, the enzyme retains cyclooxygenase activity but its peroxidase activity is significantly reduced (Streider *et al.*, 1992). This selective reduction of the peroxidase activity has only been achieved with Mn^{III}-PPIX and has been exploited to probe various aspects of PGHS mechanism, including enzyme self-inactivation (Wu *et al.*, 2001), the nature of the radical species involved in cyclooxygenase catalysis (Tsai *et al.*, 1998) and the inhibition of PGHS by poorly understood drugs such as salicylic acid and phenylbutazone (Aronoff *et al.*, 2003; Hughes *et al.*, 1988).

While the catalytic consequences of metal substitution are well characterized, the structural basis of the selective reduction of peroxidase activity by manganese substitution has remained unknown. To address this question, the 2.0 Å crystal structure of PGHS reconstituted with Mn^{III}-PPIX has

been determined. This appears to be the first structure of a protein containing an Mn^{III}-PPIX cofactor to be deposited in the Protein Data Bank.

2. Experimental procedures

Materials were obtained from the following suppliers: detergents from Anatrace (Maumee, OH, USA), flurbiprofen from Sigma Chemical (St Louis, MO, USA), Mn^{III}-protoporphyrin IX from Porphyrin Products (Logan, UT, USA), arachidonic acid from Cayman Chemical (Ann Arbor, MI, USA), ram seminal vesicles from Animal Technologies (Tyler, TX, USA) and PEG 4000, bovine hematin and other reagents from Aldrich Chemical Co. (Milwaukee, WI, USA) and Fluka (Ronkonkoma, NY, USA). All other materials were of the highest quality commercially available.

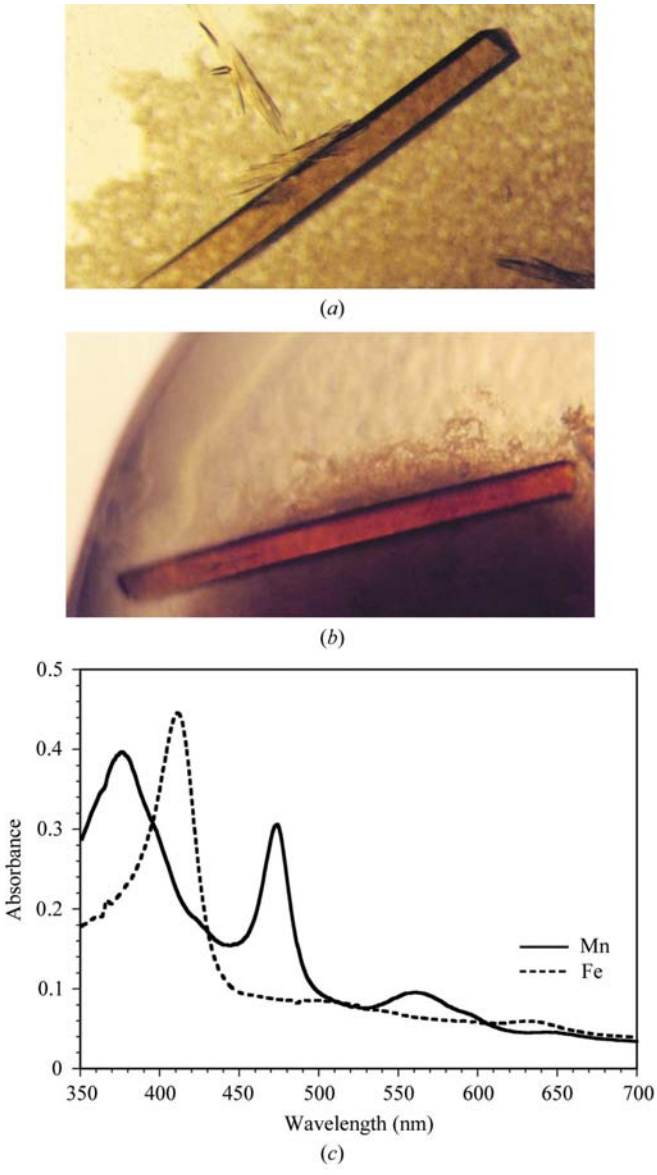

Figure 1
Crystals of (*a*) Fe-PGHS and (*b*) Mn-PGHS. In both (*a*) and (*b*) the longest dimension of the crystal shown is approximately 1 mm. (*c*) Crystal dissolution experiments. Absorption spectra are shown for dissolved crystals of Fe-PGHS (dashed line) and Mn-PGHS (solid line).

2.1. Crystallization

The apo form of ovine PGHS isoform-1 was purified from ram seminal vesicles as described previously (Gupta *et al.*, 2004). The holoenzyme was reconstituted by adding Mn^{III}-PPIX to the enzyme in a twofold molar excess at 277 K using a freshly prepared 15 m*M* porphyrin stock solution in DMSO. The protein was then concentrated to 11.5 mg ml^{-1} and dialyzed overnight at 277 K against 20 m*M* sodium phosphate pH 6.7, 50 m*M* NaCl, 0.6%(*w*/*w*) octyl glucopyranoside and 1 m*M* flurbiprofen. After dialysis, concentrated stock solutions were used to add PEG 4000 and NaCl to the protein solution; the final concentrations of PEG and NaCl fell in the ranges 1.5–3%(*w*/*w*) and 50–125 m*M*, respectively. The protein solution was then set up in hanging-drop vapor-diffusion experiments using reservoir buffers containing 4–6.5%(*w*/*w*) PEG 4000. The concentrations of sodium phosphate and NaCl in the reservoir buffer were adjusted so that the ratio of salt concentration in the protein drop to that in the reservoir matched the corresponding ratio for PEG (*e.g.* for a protein drop containing 2% PEG, 100 m*M* NaCl and 20 m*M* sodium phosphate, the reservoir buffer might contain 6% PEG, 300 m*M* NaCl and 60 m*M* sodium phosphate). Crystallization experiments were carried out at 291 K. Long reddish-brown rod-shaped crystals (0.5–1.0 × 0.1 × 0.1 mm) grew within 1–2 weeks (Fig. 1). Crystals were found over the entire range of PEG and salt concentrations used; however, large single crystals were only observed rarely and the optimal concentrations for PEG and salt varied from protein preparation to preparation. Using five steps of 5 min each, crystals were transferred from a buffer matching the drop conditions into a cryoprotectant buffer containing 30% glycerol, 7.5%(*w*/*w*) PEG 4000, 15 m*M* sodium phosphate pH 6.7, 113 m*M* NaCl, 0.4%(*w*/*w*) octyl glucopyranoside, 1 m*M* flurbiprofen and 0.1 m*M* diethyldithiocarbamic acid and were then immediately flash-cooled in liquid nitrogen.

2.2. Crystal dissolution experiments

Approximately 10–20 large single crystals of PGHS reconstituted with either Fe^{III}-PPIX or Mn^{III}-PPIX were harvested into buffers that matched the original mother liquors and were then washed by two additional transfers into fresh aliquots of buffer, allowing 5 min for each step. Crystals were then dissolved in 80 µl of 0.1 m*M* Tris pH 8.0, 0.6% octyl glucopyranoside and spectra were recorded using a Beckman DU7500 spectrophotometer.

2.3. Activity assays

Peroxidase activity was monitored using a standard colorimetric assay for H_2O_2 reduction (Kulmacz & Lands, 1987). Cyclooxygenase activity was measured by monitoring the consumption of molecular oxygen associated with the conversion of arachidonic acid to prostaglandin G_2 using a computerized Clark-style oxygen microelectrode (Instech;

Table 1
Data-collection and refinement statistics.

Values in parentheses refer to highest resolution shell.

Data collection	
Beamline	NSLS X25
Wavelength (Å)	1.099
Space group	*I*222
Unit-cell parameters (Å)	
a	98.13
b	206.55
c	221.50
Resolution (Å)	50–2.0 (2.13–2.0)
No. of observations	855595
No. of unique reflections	152014
Multiplicity	5.6 (5.6)
$R_{\rm merge}$	0.087 (0.436)
$I/\sigma(I)$	7.1 (2.4)
Completeness (%)	99.9 (100)
Refinement	
$R_{\rm cryst}$	0.218
$R_{\rm free}$	0.237
R.m.s. deviation from ideal geometry	
Bond lengths (Å)	0.007
Bond angles (°)	1.33
Dihedral angles (°)	21.9
Improper angles (°)	0.96
Ramachandran plot	
Residues in most preferred region (%)	90.1
Residues in disallowed region (%)	0.0
No. of non-H atoms in ASU	
Protein	8984
Water	892
Carbohydrate	276
Inhibitor	36
Porphyrin	84
Detergent	138
Average *B* factor, all atoms (Å^2)	33.1

Plymouth Meeting, PA, USA). In a standard assay the chamber (600 µl) contained 100 m*M* Tris–HCl pH 8.0, 1 m*M* phenol and 150 µ*M* arachidonic acid. The reactions were initiated by the addition of reconstituted enzyme.

2.4. Data collection

Diffraction data were collected at 100 K using National Synchrotron Light Source beamline X25 and an ADSC Q315 CCD detector. Data were processed using *d*TREK* (Pflugrath, 1999); data-collection statistics are shown in Table 1.

2.5. Structure solution and refinement

The starting model was derived from a 2.7 Å model of ovine PGHS-1 bound to flurbiprofen (PDB code 1eqh; Selinsky *et al.*, 2001). All refinement was performed using the *CNS* program package (Brünger *et al.*, 1998). The starting model was stripped of carbohydrate, detergent and water molecules and initial positioning of the protomer chains was achieved by rigid-body refinement using 4 Å data. Individual *B*-factor refinement and conjugate-gradient minimization were then performed iteratively using all available data. Missing features such as inhibitor, water molecules, carbohydrate and detergent were built into $F_{\rm o} - F_{\rm c}$ density iteratively using the program *O* (Jones *et al.*, 1991). Particular care was taken to ensure that the structure in the vicinity of the porphyrin group was not biased towards the starting model and much use was made of simulated-annealing omit maps (Hodel *et al.*, 1992). Because of the high resolution of the data, non-crystallographic symmetry restraints were not used during the refinement. During the latter stages of refinement, all restraints involving the manganese ion were released, while geometric restraints on the porphyrin were maintained. Finally, all restraints on the metalloporphyrin were released, which gave rise to very small changes in heme geometry and no change in R or $R_{\rm free}$ values. Anomalous difference Fourier maps using simulated-annealing omit phases were calculated to validate the position of the metal. The *CCP*4 suite of programs was used for map preparation (Collaborative Computational Project, Number 4, 1994). The final electron-density maps were of high quality throughout (Fig. 2).

3. Results

3.1. Generation and characterization of Mn^{III}-reconstituted ovine PGHS-1

The prosthetic heme group of PGHS, unlike those of many other heme peroxidases, is not covalently bound to the enzyme. The heme can, therefore, be removed during purification, allowing facile reconstitution with non-iron metalloporphyrins. After the final purification step, the protein is typically >95% apoenzyme, as determined by peroxidase assay with and without the addition of exogenous heme.

After reconstitution, the Fe^{III}- and Mn^{III}-reconstituted enzymes display distinctly different colors and absorbance spectra. A strong Soret band at 412 nm characterizes iron PGHS, while the spectrum of manganese PGHS-1 features maxima at 374, 472 and 561 nm (Streider *et al.*, 1992; Van der Ouderaa *et al.*, 1977). These spectral differences made it possible to confirm the metal substituent in crystals grown for diffraction experiments by harvesting, washing and dissolving several diffraction-quality crystals and measuring their absorbance spectra (Fig. 1).

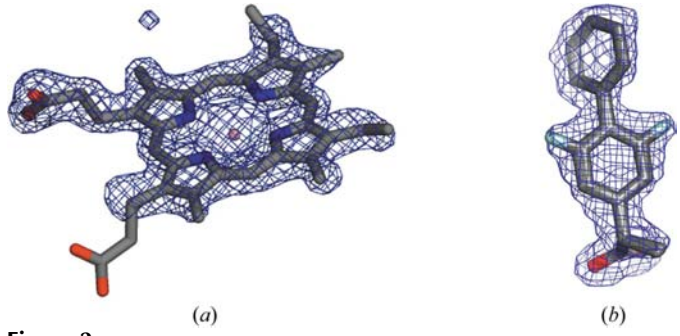

Figure 2
Simulated-annealing $2F_{\rm o} - F_{\rm c}$ omit maps calculated using phases from the final refined model. (*a*) The electron density for the porphyrin is shown superimposed on the final model. One of the propionic acid groups of the porphyrin has poor electron density and is presumed to be disordered. (*b*) Electron density for the flurbiprofen ligand. The phenyl ring of the inhibitor closer to the carboxylate acid moiety shows twofold disorder, resulting in two alternate positions for the F atoms.

The peroxidase-specific activity of manganese PGHS was found to be only 3.6% of that of the iron enzyme, as measured by the ability to reduce hydrogen peroxide in the presence of the reducing co-substrate *N*,*N*,*N*′,*N*′-tetramethylphenylenediamine (TMPD). This level of residual activity is consistent with previously reported values for the manganese form of the enzyme, which range from 0.9 to 4% (Kulmacz *et al.*, 1994; Streider *et al.*, 1992). The cyclooxygenase specific activity of Mn^{III}-PGHS was found to be comparable to that of the native enzyme and a lag phase was observed during cyclooxygenase assays, again consistent with previous reports (Streider *et al.*, 1992). Manganese PGHS crystals displayed unprecedented diffraction quality, with lower mosaicity than iron PGHS crystals and diffraction to a resolution higher than 1.9 Å (data not shown). Manganese PGHS is known to auto-inactivate more slowly than the iron enzyme (Wu *et al.*, 2001); it is possible that the higher quality of the manganese crystals may result from reduced autoinactivation prior to crystal growth.

3.2. Comparison with iron form of PGHS

Recently, a 2.0 Å crystal structure of the Fe^{III}-PPIX form of PGHS has been determined (Gupta *et al.*, 2004), allowing a direct structural comparison of the manganese and iron forms of the enzyme. The two structures are very similar, with superposition of the two models yielding overall root-mean-square differences of 0.28 Å for C^{α} positions and 0.64 Å for all atoms. These displacements are only slightly larger than the coordinate errors calculated from cross-validated Luzzati plots and σ_A plots (0.19 and 0.30 Å, respectively). The dependence of *B* values upon residue number is similar between the manganese and iron enzymes (data not shown). Residues that have been shown to affect peroxidase activity or heme binding, including His203 and Gln207 (Landino *et al.*, 1997) and Tyr504 (Seibold *et al.*, 2000), overlay each other when the two structures are superimposed, suggesting that the loss of peroxidase activity that accompanies reconstitution with Mn^{III}-PPIX does not arise from perturbation of the active site (Fig. 3). A glycerol molecule derived from the cryoprotectant binds on the distal face of the heme in both the iron and manganese structures, with one hydroxyl O atom lying near the metal; the position of the glycerol molecule does not vary between the iron and manganese structures. Residues known to affect cyclooxygenase activity, including Tyr385 (Shimokawa *et al.*, 1990), adopt the same conformations in both structures. Alternate conformations that have been identified for several residues are present in both structures at comparable occupancies. In addition, all water molecules within 8 Å of either active site are occupied similarly in both structures, indicating that the kinetic differences between the two forms of the enzyme are not traceable to differences in water binding or expulsion.

Manganese PGHS was cocrystallized with flurbiprofen, a potent cyclooxygenase inhibitor (Laneuville *et al.*, 1995). The inhibitor binds in the same site that has been identified

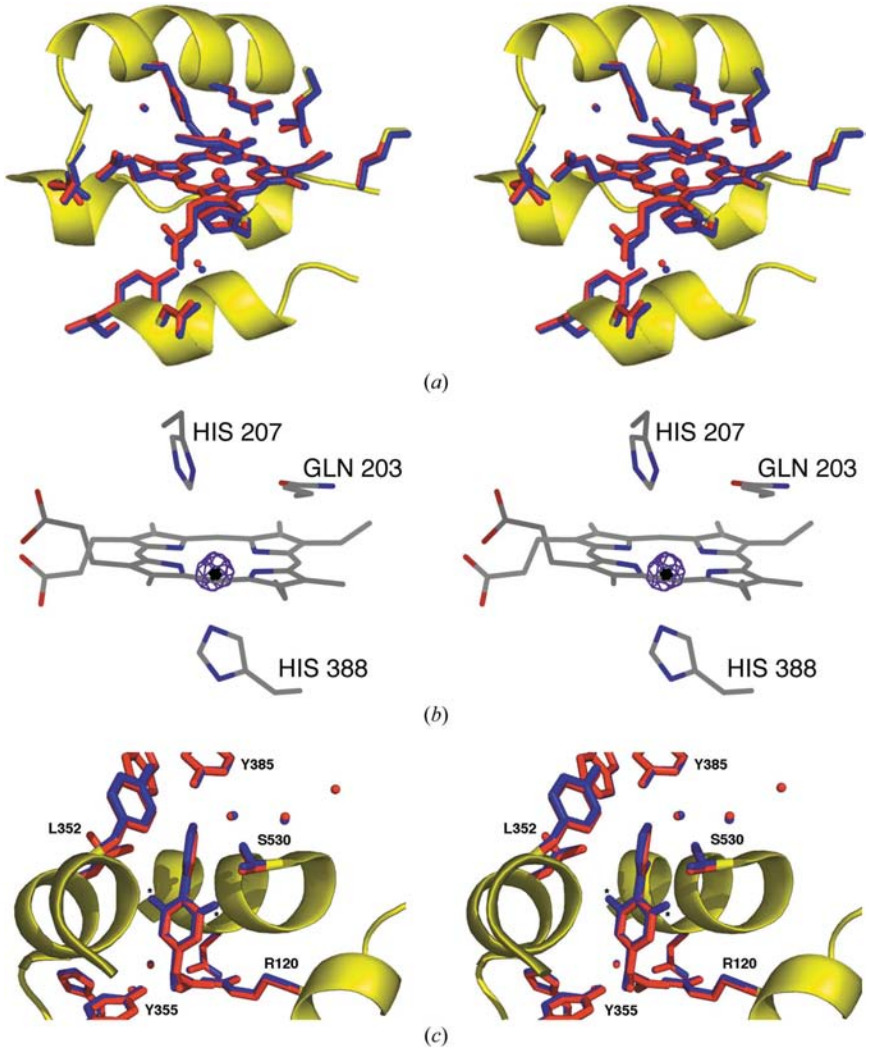

Figure 3
Stereoviews of the peroxidase and cyclooxygenase active sites. (*a*) Superposition of the peroxidase sites of the Fe-PGHS and Mn-PGHS structures. The iron structure is shown in red and the manganese structure in blue. The protein backbone is represented by the yellow ribbon. (*b*) The Mn-PGHS structure, showing the anomalous difference Fourier map contoured at 6σ. The perspective of the viewer is similar to that in (*a*), but in (*b*) the porphyrin has been rotated slightly upward about a horizontal axis relative to the orientation shown in (*a*). (*c*) Superposition of the NSAID-binding sites of the 2.0 Å Fe-PGHS and Mn-PGHS structures (Gupta *et al.*, 2004 and this work); the color scheme is the same as in (*a*). The ligand in the Fe-PGHS structure is α-methyl-4-biphenylacetic acid (desfluoro-flurbiprofen). The flurbiprofen in the Mn-PGHS structure occupies two alternate positions of roughly equal occupancy, corresponding to two alternate positions for the F atom. The two fluorine positions are marked by asterisks. Two alternate rotamers are observed for the side chain of Ser530 in both the Fe- and Mn-PGHS structures.

previously (Picot *et al.*, 1994); however, two alternate conformations are observed for the fluorinated ring of flurbiprofen, while only a single conformation was seen in earlier lower resolution structures of the Fe-PGHS–flurbiprofen complex (Selinsky *et al.*, 2001). The two conformations correspond to two orientations of the fluorinated aromatic ring rotated by 180° with respect to one another. In one orientation the F atom protrudes into a hydrophobic cleft lined by the side chains of Leu352, Phe518 and Ile523, while in the second orientation the fluorine lies close to the side chain of Ser530. The occupancies of the two fluorine positions refine to identical values. Given that no other differences are seen between the cycloooxygenase sites of the iron and manganese structures, the failure to observe multiple inhibitor conformers in the previous Fe^{III}-PPIX-PGHS–flurbiprofen structure is most likely to simply be a result of the lower resolution of the earlier structure and does not indicate any real difference in inhibitor recognition between the two forms of the enzyme.

3.3. Consequences of metal substitution in the peroxidase active site

While the positions and orientations of the protein residues comprising the peroxidase active site are essentially identical in the iron and manganese PGHS structures, there is a difference in the position of the two metal ions relative to the plane of the porphyrin ring. In the iron PGHS structure, the metal is displaced slightly out of the heme plane, toward His388; the distance from the metal to the plane formed by the four pyrrole N atoms is 0.25 and 0.29 Å, respectively, for the *A* and *B* chains. In the manganese enzyme, this displacement is more pronounced: 0.43 and 0.56 Å for chains *A* and *B*, respectively (Fig. 3). Anomalous difference Fourier maps were generated to provide an independent check on the positions of the metal atoms. The metal positions are clearly defined by sharp peaks in these maps (Fig. 3) and the peak positions are within 0.05 Å of the metal positions obtained from refinement. Thus, while small, the difference in metal positions appears to be significant and may bear mechanistic implications.

Because the crystal used for high-resolution data collection was not analyzed after irradiation, we cannot rule out that radiation damage incurred during X-ray data collection caused the metal to be reduced to Mn^{II}, which presumably would not occupy the same position as Mn^{III}. However, the position of the manganese in the 2.0 Å structure is the same as that seen in a 3.2 Å structure determined using data collected from a cryocooled crystal at a home source (data not shown). Since the radiation dose associated with the home-source data set will be much lower than that obtained at NSLS X25, this result argues against artifactual photoreduction.

The distance between the proximal histidine ligand His388 and the metal is atypically long in the iron form of PGHS (2.41 and 2.36 Å for chains *A* and *B*, respectively), reflecting an unusually weak heme ligation for a heme-dependent peroxidase (Seibold *et al.*, 2000). This bond distance is the same in the manganese enzyme (2.35 and 2.42 Å for chains *A* and *B*, respectively); the side-chain torsion angles of His388 differ slightly between the iron and manganese structures, allowing the metal–histidine distance to be maintained without backbone perturbation, despite the difference in metal positions.

The metal coordination is the same in the iron and manganese forms of PGHS, with the metal being nominally pentacoordinate (the sixth coordination site is blocked by the cryoprotectant-derived glycerol molecule). This contrasts with results reported for hemoglobin, where reconstitution with Mn^{III}-PPIX leads to loss of the water normally found at the sixth coordination position in the β-heme (Moffat *et al.*, 1976). The change from iron to manganese in the hemoglobin β-heme site is also accompanied by a marked increase in ruffling of the porphyrin. In the case of PGHS, however, out-of-plane deformations of the Mn-PPIX such as ruffling and saddling, as estimated by the *NSD* (*Normal-coordinate Structural Decomposition*) program (Jentzen *et al.*, 1997), are modest and essentially the same as those seen for the Fe-PPIX.

4. Discussion

Reconstitution with non-iron metalloporphyrins has long been used to probe mechanism in heme proteins. These alternative protoporphyrins commonly include other first-row transition metals such as manganese and cobalt, which are capable of achieving hypervalent states similar to those seen with iron. The peroxidase cycle of MnPGHS-1 proceeds through two hypervalent intermediates, Intermediates I and II, which are analogous to those formed during the peroxidase cycles of FePGHS-1; the principal kinetic difference between the manganese and iron enzymes lies in the rate of Intermediate I formation, which is much slower in the manganese enzyme (Odenwaller *et al.*, 1992; Streider *et al.*, 1992; Tsai *et al.*, 1997). This kinetic difference might result from purely electronic effects at the metal center, from structural differences, or from some combination of the two.

There are certainly intrinsic differences between iron and manganese that might lead to different catalytic properties for Fe-PGHS and Mn-PGHS. For example, model iron porphyrin compounds react significantly more rapidly with H_2O_2 than do the corresponding manganese compounds, a fact that has been ascribed to the difference in oxidation potential for the two metalloporphyrins (Balasubramanian *et al.*, 1987). Also, the addition of imidazole ligands enhances the reactivity of iron porphyrins to a considerably greater degree than for manganese porphyrins (Balasubramanian *et al.*, 1987; Labeque & Marnett, 1989). Therefore, the PGHS peroxidase active site, with its histidine proximal ligand, is likely to be better suited for amplifying the reactivity of Fe^{III}-PPIX than that of Mn^{III}-PPIX.

However, there is also a clear structural difference between iron and manganese PGHS, namely that the Mn atom is displaced farther out of the porphyrin plane toward the proximal ligand than is the iron. Since the peroxide substrate is expected to approach from the opposite, distal side of the porphyrin, this displacement has the effect of increasing the

distance between the catalytic metal and the substrate. This increased distance (~0.2 Å) is substantial relative to the length of the metal–oxygen bond that must be formed if catalysis is to proceed. This does not imply that the manganese–oxygen bond lengths in Intermediates I and II are unusual, since the metal may move closer to the porphyrin plane during the catalytic cycle; however, the initial interaction between substrate and metal must be less favorable for the manganese enzyme, simply because the metal is less accessible to the approaching peroxide.

The reasons why the manganese and iron occupy different positions are not clear. Differences in size between iron and manganese ions are small. For example, high-spin hexacoordinate Fe^{III} and Mn^{III} have identical ionic radii of 0.785 Å and the radius of low-spin hexacoordinate Mn^{III} is 0.72 Å (Shannon, 1976). Thus, the difference in metal positions cannot be explained by differences in ionic radii. It seems unlikely that the proximal histidine ligand distorts the position of the manganese, since the ligand moves with the metal, producing the same metal–ligand distances in Fe-PGHS and Mn-PGHS. In different crystal structures of manganese(III) porphyrins found in version 5.26 of the Cambridge Structural Database (Allen, 2002), the position of the metal ranges from being essentially coplanar with the pyrrole N atoms to being out of plane by as much as 0.76 Å. This suggests that the metal position is not uniquely determined by the tetrapyrrole coordination, but also reflects other environmental factors. Thus, the structural context of the PGHS heme-binding site, reflecting as it does a variety of chemical, steric and electrostatic factors, is the final determinant of the metal position. It has been proposed that the binding sites of metalloenzymes have evolved to invoke specific reduction midpoint potentials from the metals that they utilize (Vance & Miller, 1998). In the case of PGHS it appears that placing Mn-PPIX into the heme site, which as been evolutionarily 'tuned' for Fe-PPIX, leads to an unfavorable positioning of the metal.

In summary, comparison of the 2.0 Å crystal structures of Mn-PGHS and Fe-PGHS reveals a structural difference between the two forms of the enzyme, namely a metal displacement out of the porphyrin plane that is ~0.2 Å longer in the manganese enzyme. The steric hindrance introduced by this difference is expected to make the metal ion less accessible to the hydroperoxide substrate. Hence, the observed differences in catalytic behavior between the two forms of the enzyme are most likely to reflect a combination of this structural perturbation and the intrinsic differences in the redox behaviors of the two metals.

References

Allen, F. H. (2002). *Acta Cryst.* B**58**, 380–388.

Aronoff, D. M., Boutaud, O., Marnett, L. J. & Oates, J. A. (2003). *J. Pharm. Exp. Ther.* **304**, 589–595.

Balasubramanian, P. N., Schmidt, E. S. & Bruice, T. C. (1987). *J. Am. Chem. Soc.* **109**, 7865–7873.

Brünger, A. T., Adams, P. D., Clore, G. M., DeLano, W. L., Gros, P., Grosse-Kunstleve, R. W., Jiang, J.-S., Kuszewski, J., Nilges, M., Pannu, N. S., Read, R. J., Rice, L. M., Simonson, T. & Warren, G. L. (1998). *Acta Cryst.* D**54**, 905–921.

Collaborative Computational Project, Number 4 (1994). *Acta Cryst.* D**50**, 760–763.

Gupta, K., Selinsky, B. S., Kaub, C. J., Katz, A. K. & Loll, P. J. (2004). *J. Mol. Biol.* **335**, 503–518.

Hodel, A., Kim, S.-H. & Brünger, A. T. (1992). *Acta Cryst.* A**48**, 851–859.

Hughes, M. F., Mason, R. P. & Eling, T. E. (1988). *Mol. Pharmacol.* **34**, 186–193.

Jentzen, W., Song, X. Z. & Shelnutt, J. A. (1997). *J. Phys. Chem. B*, **101**, 1684–1699.

Jones, T. A., Zou, J. Y., Cowan, S. W. & Kjeldgaard, M. (1991). *Acta Cryst.* A**47**, 110–119.

Kulmacz, R. J. & Lands, W. E. M. (1987). *Prostaglandins and Related Substances. A Practical Approach*, edited by C. Benedetto, R. G. McDonald-Gibson, S. Nigam & T. F. Slater, pp. 209–227. Washington DC: IRL Press.

Kulmacz, R. J., Palmer, G., Wei, C. & Tsai, A. (1994). *Biochemistry*, **33**, 5428–5439.

Labeque, R. & Marnett, L. J. (1989). *J. Am. Chem. Soc.* **111**, 6621–6627.

Landino, L. M., Crews, B. C., Gierse, J. K., Hauser, S. D. & Marnett, L. J. (1997). *J. Biol. Chem.* **272**, 21565–21574.

Laneuville, O., Breuer, D. K., DeWitt, D. L., Hla, T., Funk, C. D. & Smith, W. L. (1995). *J. Pharm. Exp. Ther.* **271**, 927–934.

Malkowski, M. G., Theisen, M. J., Scharmen, A. & Garavito, R. M. (2000). *Arch. Biochem. Biophys.* **380**, 39–45.

Marnett, L. J., Rowlinson, S. W., Goodwin, D. C., Kalgutkar, A. S. & Lanzo, C. A. (1999). *J. Biol. Chem.* **274**, 22903–22906.

Moffat, K., Loe, R. S. & Hoffman, B. M. (1976). *J. Mol. Biol.* **104**, 669–685.

Odenwaller, R., Maddipati, K. R. & Marnett, L. J. (1992). *J. Biol. Chem.* **267**, 13863–13869.

Ogino, N., Ohki, S., Yamamoto, S. & Hayaishi, O. (1978). *J. Biol. Chem.* **253**, 5061–5068.

Pflugrath, J. W. (1999). *Acta Cryst.* D**55**, 1718–1725.

Picot, D., Loll, P. J. & Garavito, R. M. (1994). *Nature (London)*, **367**, 243–249.

Seibold, S. A., Cerda, J. F., Mulichak, A. M., Song, I., Garavito, R. M., Arakawa, T., Smith, W. L. & Babcock, G. T. (2000). *Biochemistry*, **39**, 6616–6624.

Selinsky, B. S., Gupta, K., Sharkey, C. T. & Loll, P. J. (2001). *Biochemistry*, **40**, 5172–5180.

Shannon, R. D. (1976). *Acta Cryst.* A**32**, 751–767.

Shimokawa, T., Kulmacz, R. J., DeWitt, D. L. & Smith, W. L. (1990). *J. Biol. Chem.* **265**, 20073–20076.

Simmons, D. L., Botting, R. M. & Hla, T. (2004). *Pharmacol. Rev.* **56**, 387–437.

Smith, W. L., DeWitt, D. L. & Garavito, R. M. (2000). *Annu. Rev. Biochem.* **69**, 145–182.

Smith, W. L., Garavito, M. & DeWitt, D. L. (1996). *J. Biol. Chem.* **271**, 33157–33160.

Streider, S., Schaible, K., Scherer, H. J., Dietz, R. & Ruf, H. H. (1992). *J. Biol. Chem.* **267**, 13870–13878.

Tsai, A., Palmer, G., Xiao, G., Swinney, D. C. & Kulmacz, R. J. (1998). *J. Biol. Chem.* **273**, 3888–3894.

Tsai, A., Wei, C., Baek, H. K., Kulmacz, R. J. & Van Wart, H. E. (1997). *J. Biol. Chem.* **272**, 8885–8894.

Vance, C. K. & Miller, A. F. (1998). *J. Am. Chem. Soc.* **120**, 461–467.

Van der Ouderaa, F. J., Buytenhek, M., Nugteren, D. H. & Van Dorp, D. A. (1977). *Biochim. Biophys. Acta*, **487**, 315–331.

Wu, G., Vuletich, J. L., Kulmacz, R. J., Osawa, Y. & Tsai, A. L. (2001). *J. Biol. Chem.* **276**, 19879–19888.